Polygonatum sibiricum polysaccharide alleviates liver fibrosis through the TGF-β/Smad signaling pathway and reduces collagen

YIN YUAN[1,2], XIAOJING LIU[3], TIAN ZHOU[4,5], ZHONGGUANG ZHOU[6], MINGHAI GONG[6] and YIHANG LI[1,2]

[1]Testing Center, Yunnan Branch, Institute of Medicinal Plant Development, Chinese Academy of Medical Sciences and Peking Union Medical College, Xishuangbanna Dai Autonomous Prefecture, Yunnan 666100, P.R. China; [2]Yunnan Key Laboratory of Southern Medicine Utilization, Yunnan Branch, Institute of Medicinal Plant Development, Chinese Academy of Medical Sciences and Peking Union Medical College, Xishuangbanna Dai Autonomous Prefecture, Yunnan 666100, P.R. China; [3]Department of Rehabilitation and Tuina, Liu Xin Sinew and Bone Health Center, Aksu, Xinjiang Uygur Autonomous Region 843003, P.R. China; [4]College of Basic Medical Sciences, Heilongjiang University of Chinese Medicine, Harbin, Heilongjiang 150040, P.R. China; [5]Xishuangbanna Jianlong Pharmaceutical Co., Ltd., Xishuangbanna Dai Autonomous Prefecture, Yunnan 666100, P.R. China; [6]College of Medicine, Tarim University, Alar, Xinjiang Uygur Autonomous Region 843300, P.R. China

Received February 18, 2025; Accepted May 9, 2025

DOI: 10.3892/mmr.2025.13599

Abstract. Liver fibrosis (LF) is a liver condition that represents a serious health risk to humans, and effective therapeutic options are limited. *Polygonatum sibiricum* polysaccharide (PSP), derived from the roots of *P. sibiricum* Red, has been demonstrated to exert anti-inflammatory, antioxidant and antibacterial effects. However, its potential therapeutic impact on LF remains unexplored. In the present study, LF model rats were established through subcutaneous injection of carbon tetrachloride combined with a high-fat diet and alcohol administration. Following the induction of fibrosis, rats in the PSP and Biejia ruangan (BJRG) treatment groups received daily intragastric doses of PSP and BJRG, respectively, for a duration of 4 weeks. The control and model groups were administered an equivalent volume of water. Liver function was evaluated through biochemical analyses, whereas hepatopathological alterations were assessed using hematoxylin and eosin and Masson's trichrome staining. Levels of inflammatory and oxidative stress markers were quantified using ELISA. Hepatic collagen synthesis and degradation were examined using ELISA and immunohistochemistry. Furthermore, the expression of genes and proteins associated with the TGF-β/Smad signaling pathway were analyzed by reverse transcription-quantitative PCR and western blotting. The results indicated that PSP exerts anti-fibrotic effects, primarily through anti-inflammatory and antioxidant mechanisms. Moreover, PSP appeared to promote the degradation and inhibit the synthesis of hepatic collagen fibers, potentially through modulation of the TGF-β/Smad signaling pathway.

Correspondence to: Professor Minghai Gong, College of Medicine, Tarim University, 705 Hongqiao South Road, Alar, Xinjiang Uygur Autonomous Region 843300, P.R. China
E-mail: w15663400387@163.com

Professor Yihang Li, Yunnan Key Laboratory of Southern Medicine Utilization, Yunnan Branch, Institute of Medicinal Plant Development, Chinese Academy of Medical Sciences and Peking Union Medical College, 138 Xuanwei Avenue, Xishuangbanna Dai Autonomous Prefecture, Yunnan 666100, P.R. China
E-mail: 48466685@qq.com

Key words: Polygonatum sibiricum polysaccharide, liver fibrosis, TGF-β/Smad signaling pathway, collagen, rats

Introduction

Liver fibrosis (LF) is a common pathological consequence of chronic liver injury caused by various factors. It is characterized by an imbalance between the synthesis and degradation of collagen, leading to excessive accumulation of fibrous tissue in the liver (1,2). The activation of hepatic stellate cells (HSCs) carries out a key role in the development of LF. This process occurs in three stages: i) Pre-inflammatory stage: Hepatocyte injury triggers the release of various cytokines, which promote HSC proliferation; ii) inflammatory stage: Cytokines, including platelet-derived growth factor (PDGF) and TGF-β, are secreted by Kupffer cells (KCs), sinusoidal endothelial cells, inflammatory cells and platelets, thereby stimulating HSC activation; iii) post-inflammatory stage: Activated HSCs secrete autocrine and paracrine cytokines, such as PDGF and TGF-β, further enhancing HSC activation (3,4). This cascade leads to the transformation of HSCs into myofibroblasts and the excessive production of extracellular matrix (ECM), which impairs hepatocyte function, disrupts liver architecture and ultimately contributes to the progression of LF and, potentially, liver cirrhosis (5). Therefore, inhibiting HSC activation and ECM deposition is essential for the reversal of LF.

The TGF-β/Smad signaling pathway is closely associated with the progression of LF (6). TGF-β1 initiates HSC activation by activating the Smad signaling cascade. In this

pathway, TGF-β1 binds to the TGF-β receptor (TβR) on hepatocyte membranes, leading to phosphorylation of the intracellular protein Smad3. Phosphorylated Smad3 forms a complex with Smad4, translocates to the nucleus and regulates the transcription of target genes, thus driving LF progression. Conversely, Smad7 acts as a negative regulator of the TGF-β/Smad pathway by competing with Smad3 for binding to activated TβR, thereby preventing Smad3 phosphorylation and inhibiting nuclear transcription, ultimately suppressing LF (7,8). Research has demonstrated that modulation of the TGF-β/Smad pathway can reduce carbon tetrachloride (CCl_4)-induced LF, with TGF-β also regulating ECM deposition through the modulation of matrix metalloproteinases (MMPs) (9,10). The ECM primarily comprises collagen fibers, and MMPs facilitate the breakdown of these fibers. Studies have indicated an increase in the expression of MMP2 and MMP9 in CCl_4-induced LF, which may be driven by a positive feedback mechanism (11,12).

Polygonatum sibiricum, a widely used tonic herb in China, which supports the liver, spleen and kidneys (13-15). Polysaccharides are one of the primary chemical constituents of *P. sibiricum*, which exhibit a range of pharmacological effects, such as anti-inflammatory, antioxidant, anti-aging, immune-modulating, blood glucose-lowering and lipid-regulating activities (16-20). However, the potential role of *P. sibiricum* polysaccharide (PSP) in combating LF has not been thoroughly investigated, and the involvement of mechanisms related to HSC activation and the TGF-β/Smad pathway remains unclear. Therefore, the present study aimed to explore the anti-LF effects of PSP and the mechanisms through which the TGF-β/Smad pathway mediates ECM deposition, thus providing a foundation for the development of medicinal food products targeting LF.

Materials and methods

Regents. PSP (≥98%) was obtained from Xi'an Baoyifeng Biotechnology Co., Ltd. Biejia Ruangan (BJRG) tablets were purchased from Inner Mongolia Furui Medical Science Co., Ltd. and served as a positive control drug. BJRG tablets are used in clinical practice for the treatment of LF and are commonly used as a positive control drug in the study of anti-LF in traditional Chinese medicine. The mechanism of BJRG in anti-LF is associated with the inhibition of collagen fiber synthesis and the TGF-β/Smad signaling pathway; therefore, BJRG tablets were selected as the positive control drug in the present study (21,22). High-fat diet (HFD; consisting of basic feed + 10% lard + 10% egg yolk powder + 1% cholesterol) was used in the present study (Xiaoshuyoutai Biotechnology Co., Ltd.). CCl_4 was acquired from Tianjin Tianli Chemical Co., Ltd. Olive oil was purchased from Shanghai Xinyu Biological Technology Co., Ltd. Aspartate transaminase (AST; cat. no. 04657543190), alanine aminotransferase (ALT; cat. no. 20764957322), alkaline phosphatase (ALP; cat. no. 03333752190), total bilirubin (TBIL; cat. no. 05795648190), total cholesterol (TC; cat no. 04718917190), and triglyceride (TG; cat no. 04657594190) testing kits were sourced from Roche Diagnostics. A Masson's trichrome staining kit (cat. no. MM1007) was obtained from Maokang Biotechnology Co., Ltd. TRIzol® was obtained from Invitrogen; Thermo Fisher Scientific, Inc. Taq DNA polymerase was purchased from Takara Bio, Inc. ELISA kits for hyaluronic acid (HA; cat. no. MM-0916R1), laminin (LN; cat. no. MM-0843R1), procollagen III N-terminal peptide (PIIINP; cat. no. 0752R1), collagen type IV (Col IV; cat. no. MM-70796R1), hydroxyproline (Hyp; cat no. 43761R1), α-smooth muscle actin (α-SMA; cat no. MM-61545R1), collagen type I (Col I; cat no. MM-0041R1), collagen type III (Col III; cat no. MM-0080R1), IL-1β (cat no. MM-0047R1), TNF-α (cat no. MM-0180R1), IL-10 (cat no. MM-0195R1), superoxide dismutase (SOD; cat no. MM-0386R1), malondialdehyde (MDA; cat no. MM-0576R1) and glutathione peroxidase (GSH-PX; cat no. 0743R1) were purchased from Jiangsu Enzyme Immunoassay Co., Ltd. Goat serum (cat. no. c-0005), MMP2 (cat. no. bs4605R), MMP9 (cat. no. bsm55544m), Col III (cat no. bs-0549R) and Col I (cat no. bs-7158R) antibodies were obtained from Bioss. RIPA lysis buffer (cat. no. c1053) was purchased from Applygen Technologies, Inc. TGF-β1 (cat. no. ab215715), Smad3 (cat. no. ab40854) and Smad7 (cat. no. ab216428) antibodies were acquired from Abcam Co., Ltd. HRP-labeled secondary antibody (cat. no. 111005003) was purchased from Jackson ImmunoResearch Laboratories, Inc. The anti-GAPDH antibody (cat. no. AF1186) and enhanced chemiluminescent reagents (ECL; cat no. P0018FSwere obtained from Beyotime Institute of Biotechnology.

Animal experiments. A total of 70 male Sprague Dawley (SD) rats (weight, 180-220 g; age, 6 weeks) were obtained from Liaoning Changsheng Biotechnology Co., Ltd. [animal production license no. SCXK (Liao) 2020-002]. The rats were housed in a specific pathogen-free environment with a 12-h light/dark cycle, a relative humidity of 50±5% and a room temperature of 22±2˚C. The control group consisted of 10 rats, while the other groups had 8 rats each. A total of 10 male SD rats were randomly assigned as the control group receiving standard feed and purified water *ad libitum*, whereas the remaining rats (n=60 SD rats) underwent LF induction through a 7-week protocol comprising: i) HFD administered twice daily (150-200 g/feeding) and *ad libitum* access to purified water; ii) daily 20% ethanol gavage (10 ml/kg; prepared from 56% alcohol by volume) and iii) subcutaneous CCl_4 injections (initial 5 ml/kg; followed by 3 ml/kg 40% CCl_4 in olive oil every 3 days for 14 total injections) (23). Control group rats received equivalent olive oil injections. Rats were randomly divided into the model group, BJRG group (administered 1.70 g/kg BJRG), PSP_L group (administered 0.80 g/kg PSP) or PSP_H group (administered 1.60 g/kg PSP). All groups consisted of 10 rats each. The control and model groups received a daily oral gavage of purified water (10 ml/kg), whereas treatment groups were intragastrically administered either PSP aforementioned doses or BJRG tablets (positive control drug) at the same volume and frequency for 4 weeks. The Chinese Pharmacopoeia stipulates a daily dosage range of 9-15 g *P. sibiricum* for adult human use (24) For the experimental design of the present study, a maximum recommended human dose of 15 g/day was used as the reference point. Through interspecies dose conversion based on body surface area normalization, the equivalent dose in a rat was calculated to be 1.35 g/kg/day. Considering a crude polysaccharide extraction efficiency of ~60% from

the raw herb, the daily administration dose of PSP for rats was calculated as 0.8 g/kg/day, which was designated as the medium dose (MD) in the protocol of the present study. The high dose group received 1.6 g/kg/day (2X the MD), while the low dose group was administered 0.4 g/kg/day (0.5X the MD). Preliminary investigations demonstrated that the 0.4 g/kg/day dose failed to elicit significant therapeutic effects in the LF rat model. Consequently, formal investigation focused on the two higher doses, ultimately selecting 0.8 and 1.6 g/kg/day for comprehensive evaluation in the present study. On the final day of the present study, the rats were anesthetized with 3% sodium pentobarbital (40 mg/kg; intraperitoneal injection). After confirming surgical anesthesia (loss of righting/pedal reflexes), blood was collected via abdominal aortic puncture (7-10 ml from each rat) and the liver samples were surgically resected. After tissue collection, the rats were euthanized by cervical dislocation. Death was confirmed by cardiac arrest, respiratory cessation (≥5 min) and rigor mortis. A portion of the liver tissue was fixed in 4% paraformaldehyde for 24 h at room temperature for histological analysis, while the remaining tissue was stored at -80˚C. All animal procedures were approved by the Animal Ethics Committee of Heilongjiang University of Chinese Medicine (approval no. 2021101101; Harbin, China).

Liver index. The livers were washed with saline and swabbed dry, weighed on an analytical balance, liver weights were recorded and images were captured. Liver index (%) was calculated using the formula=liver weight/body weight x100.

Biochemical testing. Following anesthesia, blood was drawn from the abdominal aorta and allowed to stand for 2.5 h. The supernatant (serum) was carefully collected after centrifugation at 3,010 x g for 15 min at 4˚C. ALT, AST, ALP, TBIL, TC and TG test kits were used according to the manufacturers' instructions. The serum samples were placed in the designated wells, and an automatic biochemical analyzer (Roche Diagnostics) was used to measure the levels of ALT, AST, ALP, TC and TG.

Hematoxylin and eosin (H&E) and Masson's trichrome staining. Liver tissues were fixed in 4% paraformaldehyde for 24 h at room temperature, dehydrated through a graded ethanol series [50% (45 min), 70% (45 min), 80% (45 min), 90% (45 min), 95% (45 min), 100% ethanol I (30 min) and 100% ethanol II (20 min)], cleared in xylene (twice, 30 min each) and embedded in paraffin wax at 65˚C. Sections (4 μm) were cut for deparaffinization. The slides were sequentially immersed in xylene I (10 min), xylene II (10 min), 100% ethanol I (2 min), 100% ethanol II (2 min), 95% ethanol (2 min), 90% ethanol (2 min) and 80% ethanol (2 min), and then rinsed thoroughly in distilled water (4 min). Subsequently, the tissues were subjected to H&E or Masson's trichrome staining for ~2 h at room temperature. The stained sections were examined under an optical microscope (Motic Incorporation, Ltd.). Relative statistical analysis of Masson-stained collagen fiber deposition was carried out using ImageJ 1.54f software (National Institutes of Health). Meta-analysis of Histological Data in Viral Hepatitis (METAVIR) scores were used to evaluate LF (25).

Immunohistochemical staining. Paraffin-embedded sections (4 μm) were dewaxed twice using xylene, followed by gradient ethanol hydration and antigen retrieval using sodium citrate solution at 100˚C. To inhibit endogenous peroxidase activity, the sections were treated with 3% hydrogen peroxide for 20 min at room temperature. Subsequently, the sections were blocked with goat serum for 20 min at room temperature and incubated overnight at 4˚C with primary antibodies targeting MMP2 (1:150), MMP9 (1:200), Col III (1:200) and Col I (1:500). On the following day, the sections were incubated with appropriate HRP-labelled secondary antibodies (1:1,000) for 30 min at room temperature. Protein expression was visualized using 3'-diaminobenzidine staining, after which the sections were counterstained with hematoxylin for 50 sec at room temperature and examined under an optical microscope (Motic Incorporation, Ltd.). Using the ImageJ 1.54f software, the integrated optical density values of positively expressed cells in each group were calculated.

ELISA. Following anesthesia, blood was drawn from the abdominal aorta and allowed to stand for 2.5 h. The supernatant was carefully collected after centrifugation at 805 x g for 15 min at 4˚C. The serum levels of HA, LN, PIIINP Col IV, IL-1β, TNF-α, IL-10, SOD, MDA and GSH-PX were determined by ELISA according to the manufacturer's instructions.

In addition, to measure hepatic Hyp, Col I, Col III and α-SMA contents, 0.1 g liver tissues were homogenized with 900 μl ice-cold PBS using a glass homogenizer on crushed ice until complete tissue disruption was achieved. The homogenate was centrifuged at 3,010 x g for 15 min in a refrigerated centrifuge (4˚C) to remove cellular debris. The supernatant was then collected and hepatic Hyp, Col I, Col III and α-SMA contents were measured using ELISA kits according to the manufacturer's protocols.

Reverse transcription-quantitative PCR. Total RNA was isolated from liver tissues using TRIzol, according to the manufacturer's instructions. cDNA synthesis was carried out using a two-step method with a prime script RT reagent kit (Takara Bio, Inc.) at 37˚C for 15 min and 85˚C for 5 sec. qPCR was performed using the TB green premix kit (Takara Bio, Inc.) under the following conditions: i) Initial denaturation: 95˚C for 30 sec (1 cycle); ii) Amplification: 40 cycles of 95˚C for 5 sec and 60˚C for 30 sec; iii) Melt curve analysis: 65˚C to 95˚C with 0.5˚C increments (5 sec/step). Cycle thresholds were normalized to GAPDH levels in the same sample. The $2^{-\Delta\Delta Cq}$ method was employed to analyze the mRNA data (26), and the expression levels are presented as fold changes relative to GAPDH. The sequences of the primers used are provided in Table I.

Western blotting. Proteins were extracted from liver tissue using RIPA buffer. Protein concentrations were determined using the BCA assay (Beyotime Institute of Biotechnology) according to the manufacturer's protocol. A total of 10 μg protein/lane was separated by SDS-PAGE on 10% gels, followed by transfer to a PVDF membrane (MilliporeSigma). The membranes were blocked with 5% non-fat dried milk for 2 h at room temperature and washed three times with 1X TBS-0.1%Tween, then incubated overnight at 4˚C with primary antibodies against TGF-β1

Table I. Primer sequences for reverse transcription-quantitative PCR.

Gene name	Forward primer, 5'-3'	Reverse primer, 5'-3'
TGF-β1	CATGGAGCTGGTGAAACGGAAG	GACTGGCGAGCCTTAGTTTGGAC
Smad3	TGCTACCTCCAGTGTTGGT	GCGGGGAAGTTAGTGTTCT
Smad7	GGTGCGTGGTGGCATACT	GCTGACTCTTGTTGTCCGAAT
GAPDH	GATGACATCAAGAAGGTGGTGA	ACCCTGTTGCTGTAGCCATATTC

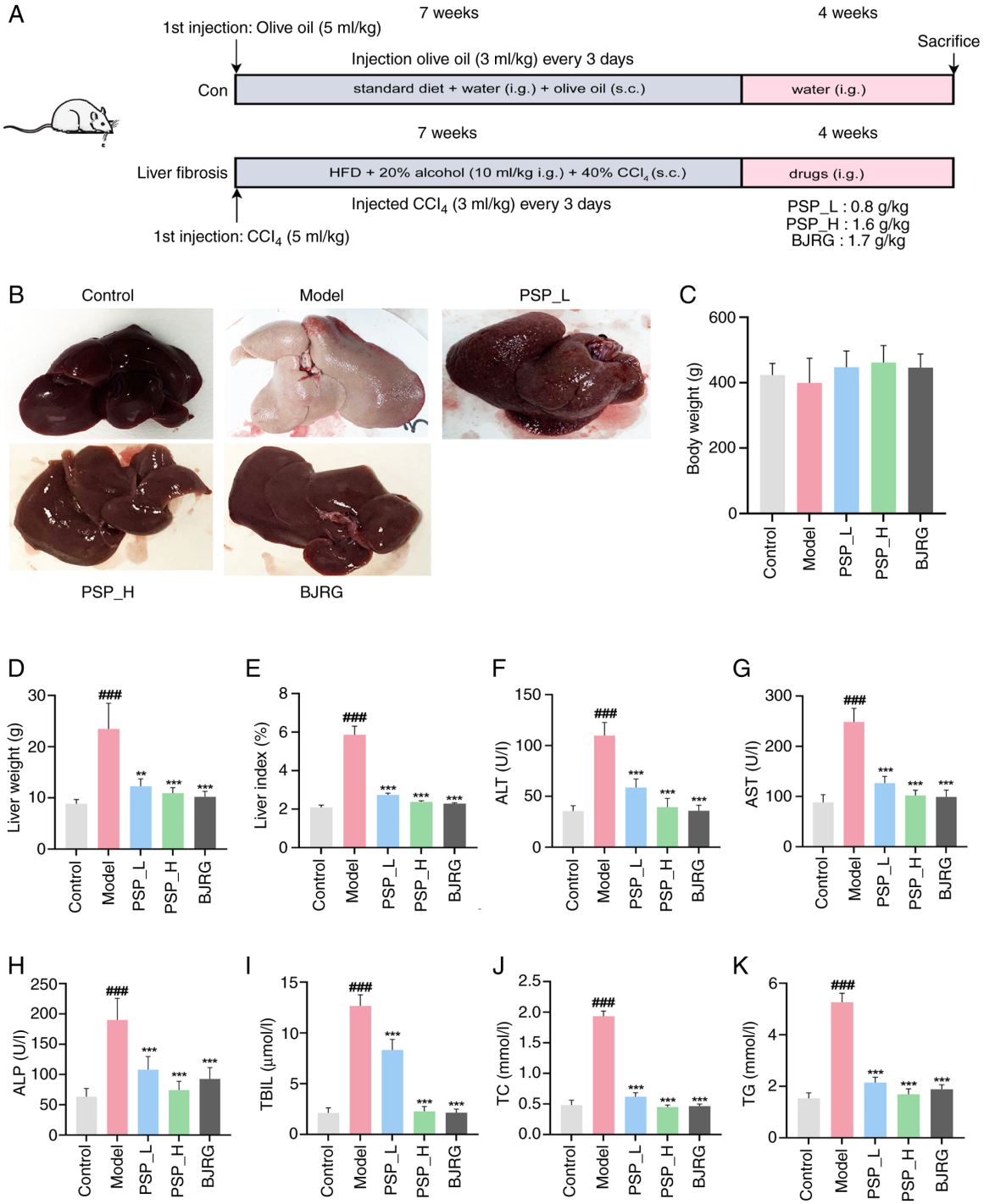

Figure 1. PSP has an anti-LF effect. (A) Workflow chart of the experiment used to assess the anti-LF effects of PSP. (B) Images of the liver. (C) Body weight of rats at end of the experiment. (D) Liver weight. (E) Liver index. Serum biochemical analyses of (F) ALT, (G) AST, (H) ALP and (I) TBIL, assessing liver function. Serum biochemical analyses of (J) TC and (K) TG, assessing blood lipid. Data are presented as the mean ± standard deviation, n=6. $^{###}$P<0.001 vs. the control group; **P<0.01, ***P<0.001 vs. the model group. ALP, alkaline phosphatase; ALT, alanine aminotransferase; AST, aspartate transaminase; CCl_4, carbon tetrachloride; H, high; L, low; LF, liver fibrosis; PSP, *Polygonatum sibiricum* polysaccharide; TBIL, total bilirubin; TC, total cholesterol; TG, triglyceride.

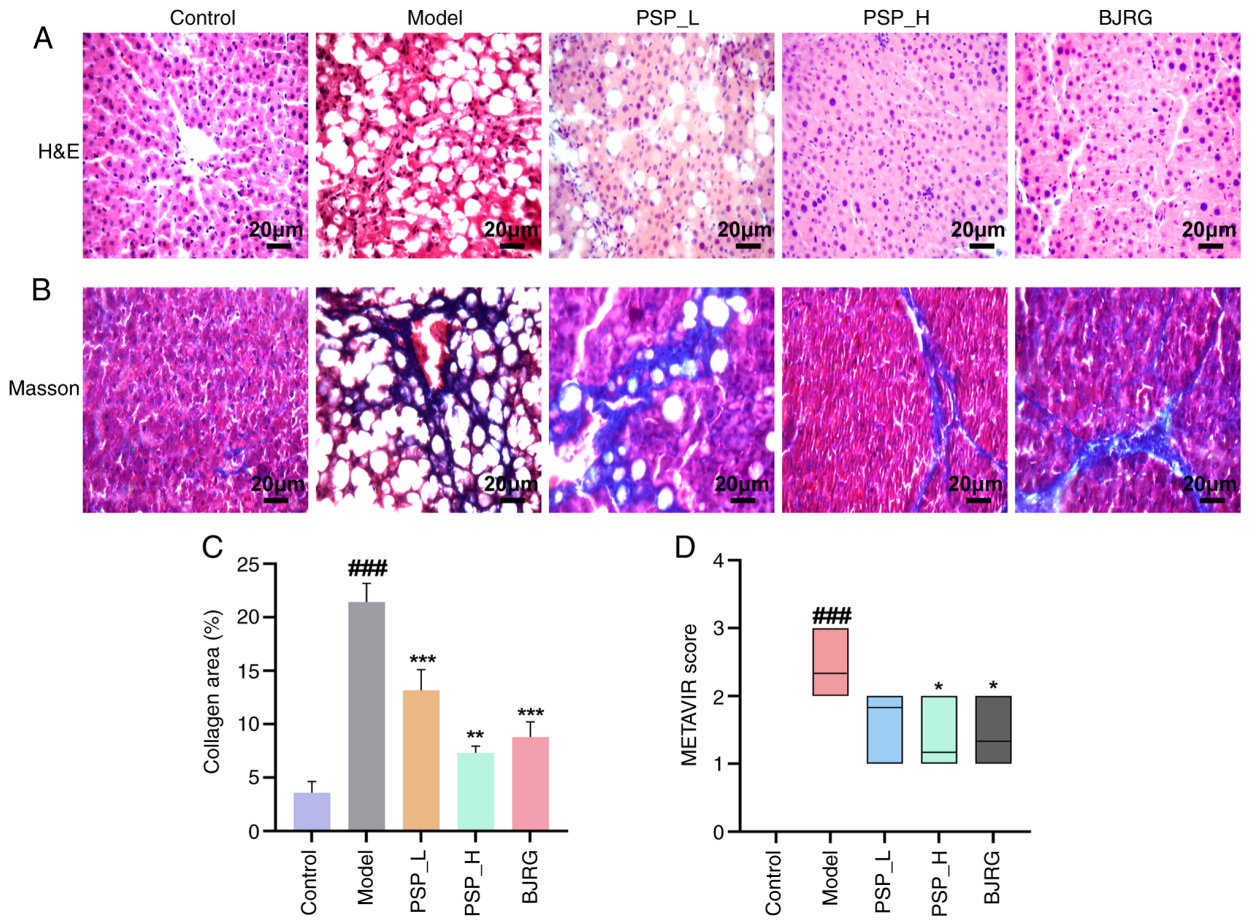

Figure 2. PSP attenuates hepatic pathological structural changes presented by rats with liver fibrosis. (A) H&E staining and (B) Masson's trichrome staining were performed to observe the liver tissue structure; scale bar, 20 μm. (C) Liver collagen fiber deposition ratio. (D) Hepatic METAVIR scores. Data are presented as the mean ± standard deviation, n=6. $^{###}$P<0.001 vs. the control group; *P<0.05, **P<0.01 and ***P<0.001 vs. the model group. BJRG, Biejia ruangan; H, high; H&E, hematoxylin and eosin; METAVIR, Histological Data in Viral Hepatitis; L, low; PSP, *Polygonatum sibiricum* polysaccharide.

(1:500), Smad3 (1:1,000), Smad7 (1:1,000), and GAPDH (1:1,000). The following day, the membranes were incubated with HRP-labelled secondary antibodies (1:10,000) for 1 h at room temperature. After applying the ECL working solution evenly onto the protein bands, the bots were incubated in the dark for 5 min at room temperature, and were detected using a gel imaging system (Tanon Science and Technology Co., Ltd.). The gray values were normalized to those of GAPDH and were semi-quantified using ImageJ 1.54f software.

Statistical analysis. The data were analyzed using GraphPad Prism 9.0 software (Dotmatics) and are presented as the mean ± standard deviation. The METAVIR score was analyzed using Kruskal-Wallis test and Dunn's post hoc test. One-way ANOVA was used for comparisons between groups when the data followed a normal distribution, with Dunnett's method applied for post hoc analyses when the variance was homogeneous, and Tamhane T2 method was used when the variance was heterogeneous. P<0.05 was considered to indicate a statistically significant difference.

Results

PSP improves liver function in rats with LF. To initially evaluate the anti-LF effects of PSP, LF model rats were fed a HFD combined with alcohol and CCl_4. After modeling, the rats were given PSP for 4 weeks (Fig. 1A). The overall liver condition and function were subsequently assessed. The liver in the model group appeared enlarged, yellowish and dull in color, with a greasy texture, rough surface, visible particles of varying sizes, a slightly firm texture and blunted margins (Fig. 1B). The livers of rats treated with PSP or BJRG revealed decreased liver volume, a healthy red color, non-greasy texture, smooth surface, reduced number of particles and a soft texture. Additional testing revealed that the liver weight, liver index and levels of biochemical markers (ALT, AST, ALP, TBIL, TC and TG) in the model group were significantly higher compared with those in the control group (Fig. 1C-K). However, following treatment with PSP or BJRG, these parameters were significantly decreased compared with those in the model group, suggesting that PSP may exert anti-LF effects.

PSP attenuates liver injury in rats with LF. Collagen deposition and structural disorganization of the liver lobules are typical pathological features of LF (27). To further evaluate the effect of PSP on LF, liver tissue histology was examined using H&E and Masson's trichrome staining. H&E staining revealed disruption of the liver lobule structure in the model group, with hepatocytes arranged irregularly, marked focal necrosis, nuclear atrophy, extensive steatosis, inflammatory

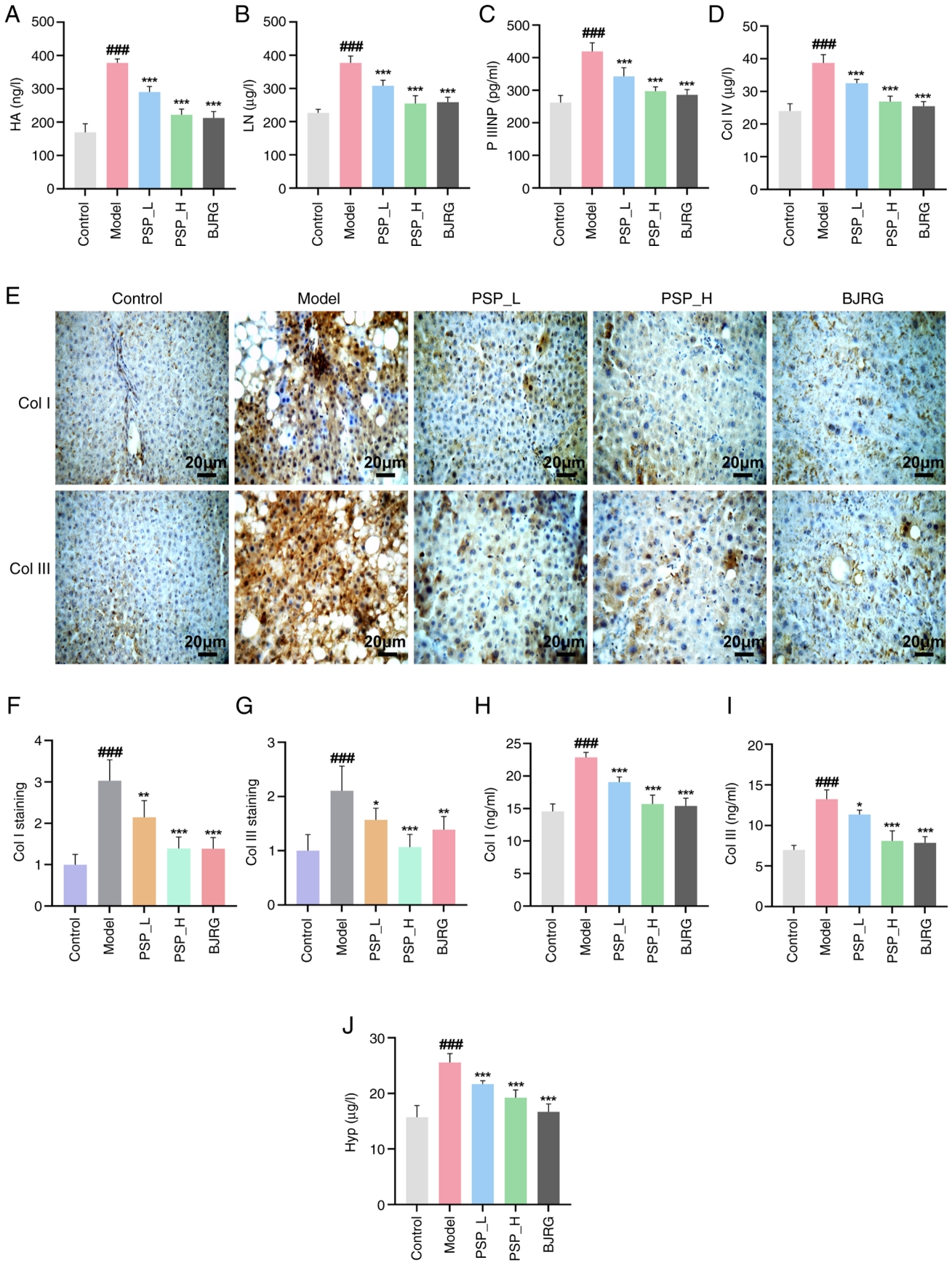

Figure 3. PSP inhibits hepatic collagen production in liver fibrosis-induced rats. Detection of the liver fibrosis markers (A) HA, (B) LN, (C) PIIINP and (D) Col IV in serum samples was performed by ELISA. (E) Expression levels of Col I and Col III in the liver were detected by immunohistochemistry; scale bar, 20 μm. Semi-quantification of (F) Col I and (G) Col III. ELISA was used to detect the levels of (H) Col I and (I) Col III in liver tissue. (J) Levels of Hyp in the liver tissues were detected by ELISA. Data are presented as the mean ± standard deviation, n=6. $^{###}$P<0.001 vs. the control group; *P<0.05, **P<0.01 and ***P<0.001 vs. the model group. BJRG, Biejia ruangan; Col, collagen; H, high; HA, hyaluronic acid; Hyp, hydroxyproline; L, low; LN, laminin; PIIINP, procollagen III N-terminal peptide; PSP, *Polygonatum sibiricum* polysaccharide.

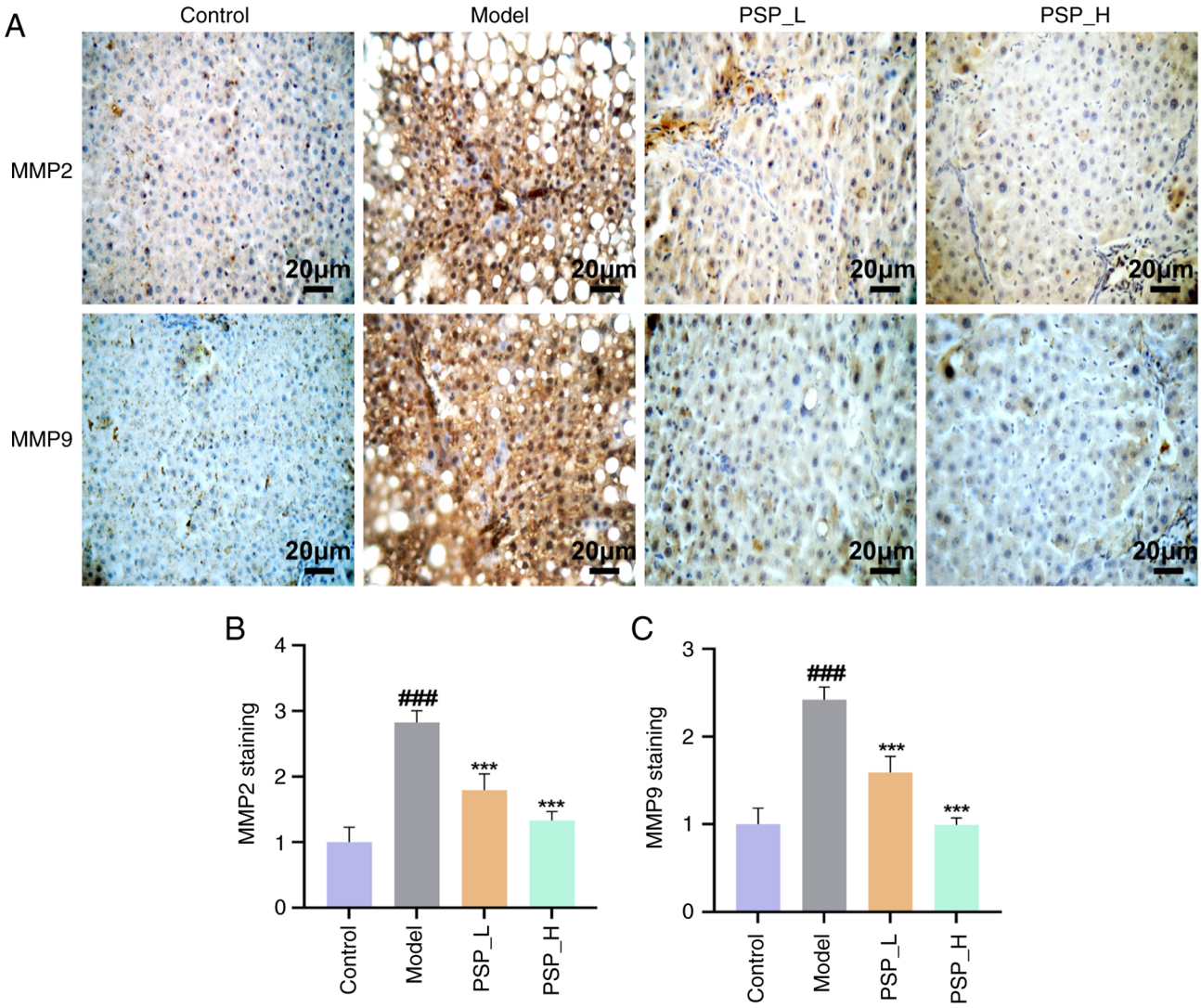

Figure 4. PSP promotes hepatic collagen fiber breakdown in liver fibrosis model rats. (A) Expression levels of MMP2 and MMP9 in the liver were assessed using immunohistochemistry; scale bar, 20 μm. Relative expression levels of (B) MMP2 and (C) MMP9. Data are presented as the mean ± standard deviation, n=6. $^{###}$P<0.001 vs. the control group; ***P<0.001 vs. the model group. BJRG, Biejia ruangan; H, high; L, low; PSP, *Polygonatum sibiricum* polysaccharide.

cell infiltration and fibrous hyperplasia (Fig. 2A). For samples treated with PSP or BJRG, the liver lobules presented a more organized structure, and hepatocytes had a more regular morphology and size, with only mild disorganization in the arrangement, no steatosis or focal necrosis, reduced inflammatory cell infiltration and almost no fibrous hyperplasia.

Masson's trichrome staining revealed that the model group exhibited extensive deposition of interconnected collagen fibers, primarily localized in portal confluence areas and perivenular regions, with progressive extension into hepatic lobules forming irregularly thickened fibrous septa, accompanied by severe steatosis and hepatocellular necrosis (Fig. 2B). By contrast, treatment with either PSP or BJRG attenuated these pathological changes, demonstrating a reduction of collagen deposition in portal confluence zones, marked suppression of fibrous septum formation and concurrent alleviation of steatosis and necrotic lesions. Meanwhile, hepatic collagen fiber area and Metavir scores were significantly increased in the model group compared with those in the control group (Fig. 2C and D). PSP and BJRG treatment significantly reduced both collagen deposition and Metavir scores. These results indicated that PSP exerts potent anti-fibrotic effects possibly through targeted modulation of collagen remodeling and hepatoprotective mechanisms.

PSP inhibits hepatic collagen production in rats with LF. HA, LN, PIIINP and Col IV are key serum markers used in diagnosing LF, and their levels markedly rise during LF (28). The present results demonstrated that the serum levels of HA, LN, PIIINP and Col IV were significantly elevated in the model group compared with those in the control group; however, these serum levels were markedly reduced in groups treated with PSP or BJRG (Fig. 3A-D). To further assess collagen synthesis in liver tissue, the levels of Hyp were measured. Analysis revealed significantly increased Hyp levels in the liver tissue of the model group compared with those in the control group; however, treatment with PSP or BJRG led to a significant reduction in Hyp content compared with that in the model group (Fig. 3J). Moreover, the levels of Col I and

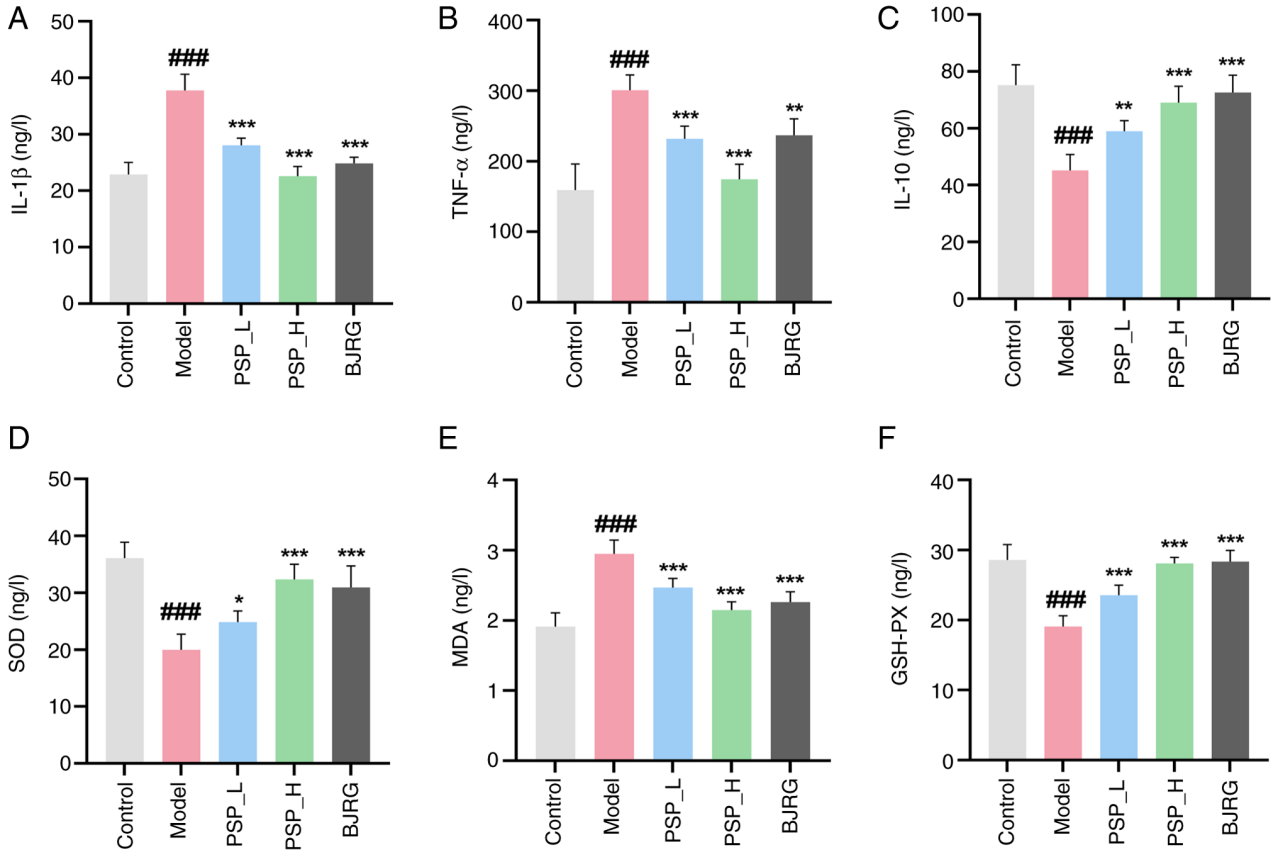

Figure 5. PSP attenuates inflammatory response and oxidative stress in liver fibrosis model rats. Levels of (A) IL-1β, (B) TNF-α (C) and IL-10 in the serum were analyzed by ELISA. Detection of serum levels of (D) SOD, (E) MDA (F) and GSH-PX was performed using ELISA. Data are presented as the mean ± standard deviation, n=6. $^{###}$P<0.001 vs. the control group; *P<0.05, **P<0.01 and ***P<0.001 vs. the model group. BJRG, Biejia ruangan; GSH-PX, glutathione peroxidase; H, high; L, low; MDA, malondialdehyde; PSP, *Polygonatum sibiricum* polysaccharide; SOD, superoxide dismutase.

Col III in the liver, the primary collagen types in the liver, were significantly increased in the model group compared with those in the control group (Fig. 3E-I). By contrast, treatment with PSP and BJRG resulted in decreased expression of Col I and Col III. Notably, PSP inhibited the expression of collagen synthesis-related factors and proteins. Overall, PSP was revealed to inhibit hepatic collagen production in LF rats.

PSP promotes hepatic collagen fiber breakdown in LF model rats. MMP2 and MMP9 are key proteins involved in the degradation of Col IV. In LF, the integrity of the vascular basement membrane serves a crucial role and Col IV is the main collagen in the vascular basement membrane (29). Our previous studies revealed significantly elevated levels of Col IV in the serum of LF, but the underlying mechanism remains unclear. To explore the effect of PSP on the vascular basement membrane in LF model rats, the expression of MMP2 and MMP9 was assessed in liver tissue. The results revealed that the protein expression levels of MMP2 and MMP9 were significantly increased in the model group compared with those in the control group; however, treatment with PSP or BJRG led to a significant decrease in the expression of MMP2 and MMP9 (Fig. 4A-C). These findings suggested that PSP might protect the integrity of the basement membrane by reducing MMPs.

PSP attenuates the inflammatory response and oxidative stress in rats with LF. LF is often accompanied by inflammation and oxidative stress, where the levels of proinflammatory factors (IL-1β and TNF-α) and peroxidation markers (MDA) are elevated, whereas the levels of anti-inflammatory (IL-10) and antioxidant factors (SOD and GSH-PX) are reduced (30). Pathological analysis of the liver revealed a notable inflammatory response in the model group compared with in the control group. The findings indicated that the serum levels of IL-1β, TNF-α and MDA were significantly elevated in the model group compared with those in the control group (Fig. 5A, B and E). By contrast, the levels of IL-10, SOD and GSH-PX were significantly reduced compared with those in the control group (Fig. 5C, D and F). However, treatment with PSP or BJRG markedly reduced the levels of IL-1β, TNF-α and MDA, while substantially increasing the levels of IL-10, SOD and GSH-PX. These results suggested that PSP may effectively alleviate the inflammatory response and oxidative stress in rats with LF.

PSP-mediated modulation of the TGF-β/Smad signaling pathway has anti-LF effects. In the development of LF, the TGF-β/Smad signaling pathway serves a key role, since the activation of HSCs promotes the release of TGF-β1. To investigate whether PSP affects the TGF-β/Smad pathway and contributes to the reduction in LF, levels of α-SMA and other components of the TGF-β/Smad pathway were assessed. PSP and BJRG treatment significantly reduced α-SMA expression

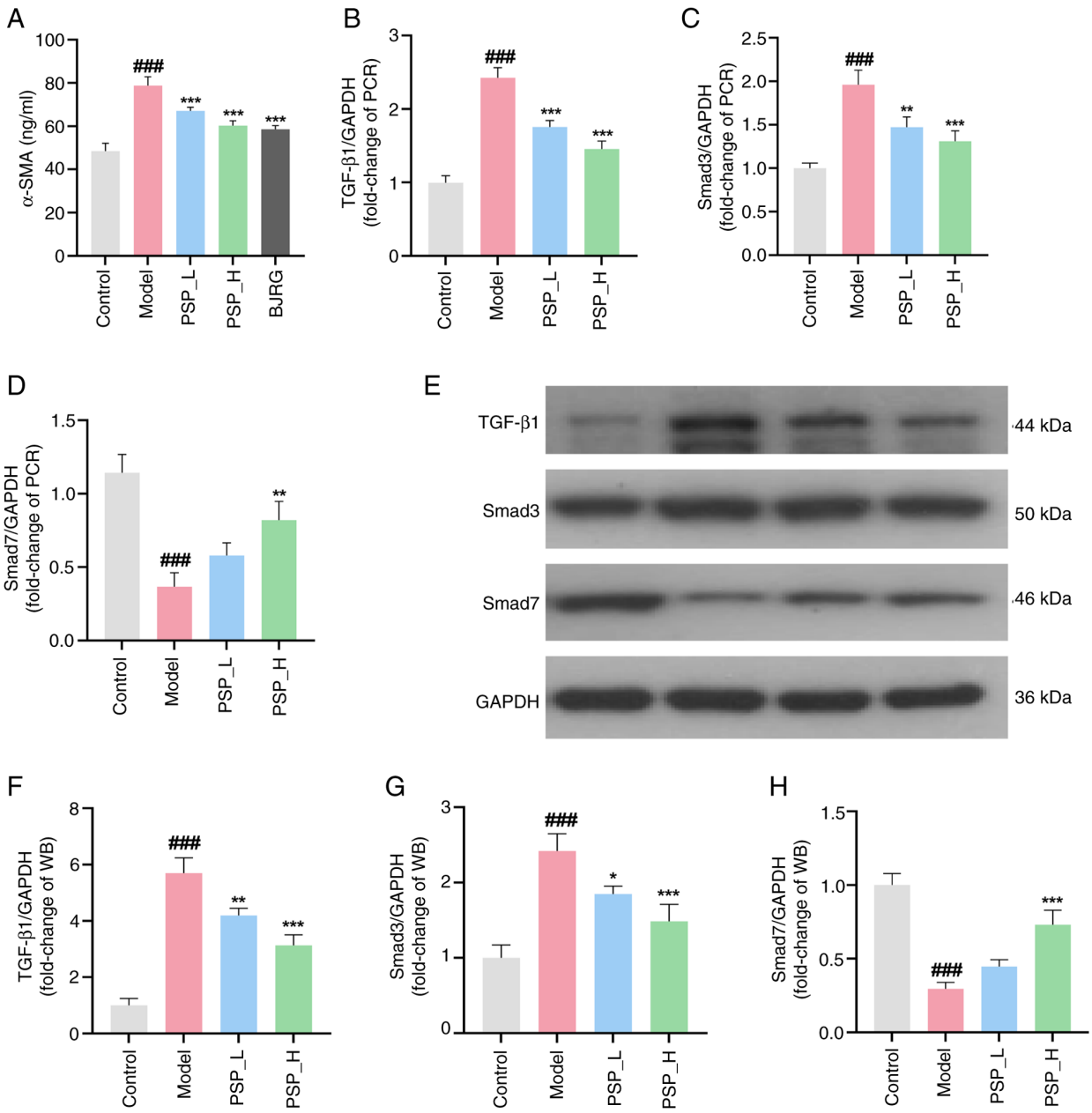

Figure 6. PSP-induced modulation of the TGF-β/Smad signaling pathway exerts anti-liver fibrosis effects. (A) The level of α-SMA in liver tissue by ELISA assay. mRNA expression of (B) TGF-β1, (C) Smad3 and (D) Smad7 by reverse transcription-quantitative PCR. (E) Representative western blotting images, and protein expression levels of (F) TGF-β1, (G) Smad3 and (H) Smad7. Data are presented as the mean ± standard deviation, n=3. $^{###}$P<0.001 vs. the control group; *P<0.05, **P<0.01 and ***P<0.001 vs. the model group. α-SMA, α-smooth muscle actin; BJRG, Biejia ruangan; H, high; L, low; PSP, *Polygonatum sibiricum* polysaccharide.

levels in liver tissue, suggesting potential inhibition of HSC activation (Fig. 6A). Furthermore, the protein and mRNA levels of TGF-β1 and Smad3 were significantly elevated in the model group compared with those in the control group, whereas Smad7 levels were notably decreased (Fig. 6B-H). By contrast, following treatment with PSP, the expression of TGF-β1 and Smad3 was reduced, whereas Smad7 expression levels were significantly increased.

Discussion

LF results from a reparative response involving ECM deposition driven by the activation of HSCs (31). During the repair of acute liver injury, parenchymal cells regenerate to replace damaged or dead cells, a process characterized by inflammation, oxidative stress and ECM accumulation. If liver injury persists, hepatocyte regeneration is impaired, and excessive ECM, including collagen, replaces hepatocytes (32,33). *P. sibiricum*, a source of Chinese medicine known to have medicinal effects (34), contains polysaccharides as its main component. Daily administration of 0.15, 0.3 or 0.45 g/kg PSP via oral gavage in rats has been shown to improve CCl_4-induced hepatotoxicity, indicating its safety and efficacy at these doses (35). Pharmacokinetic studies have revealed that 0.1 g/kg PSP is distributed to the majority of tissues within 8 h of oral administration in rats,

with the highest concentrations found in the kidney, liver and lung (36,37). These findings suggest that the liver may be the primary organ for metabolism and the target organ for PSP. In the present study, administering 0.8 or 1.6 g/kg/day PSP daily via oral gavage improved liver function, inhibited lipid accumulation and decreased collagen deposition in rats with HFD-induced LF. These findings suggested that PSP may have anti-fibrotic effects on LF.

Ongoing injury to blood vessels caused by LF results in the breakdown of the vascular basement membrane and increases the production of markers associated with LF, which then enter the bloodstream (38). Serum levels of HA, LN, PIIINP and Col IV are notably higher in individuals with LF (39-41). In the present study, a significant increase in the serum levels of HA, LN, PIIINP and Col IV was observed in the LF model group compared with those in the control group. This may indicate substantial disruption of the hepatic vascular basement membrane, allowing these markers to enter the bloodstream. Furthermore, PSP significantly decreased serum marker levels, although whether this contributes to repair of the vascular basement membrane or inhibits the production of LF markers requires further investigation.

ECM deposition can increase intrahepatic blood flow resistance, leading to the formation of pseudolobules. This process may progress to portal hypertension, cirrhosis and potentially hepatocellular carcinoma (42,43). Therefore, limiting the excessive deposition of ECM is a key strategy for combating LF. The ECM in the liver primarily consists of collagen types I, III, IV, V and VI. Col I and Col III account for ~80% of the total intrahepatic collagen, with a predominant distribution in the portal triad (44). In LF, the levels of collagen types I and III are elevated, particularly Col I, which constitutes 70-80% of the total collagen in cirrhotic tissues and serves as a significant marker of advanced LF and cirrhosis (45-47). The results of the present study indicated that PSP notably decreased the deposition of Col I in the liver.

Hyp, a key amino acid involved in collagen synthesis, serves as a direct indicator of collagen content (48). To assess whether PSP inhibits collagen synthesis, the Hyp content was measured and found to be significantly reduced in liver tissue following PSP treatment. These results suggested that PSP may decrease ECM deposition in the liver; however, it is not yet clear the effect of PSP on collagen fibers in the hepatic vascular basement membrane. To investigate this, the collagenase enzymes MMP2 and MMP9, which are key for collagen breakdown, were examined. MMP2 and MMP9 mainly degrade Col IV in the basement membrane. In LF, the expression levels of MMP2 and MMP9 in the liver are elevated (49), which promotes the degradation of vascular basement membrane Col IV and leads to vascular endothelial damage. The resulting Col IV fragments are subsequently released into the bloodstream, causing an increase in circulating Col IV levels, which aligns with the findings of the present study. In the current study, PSP significantly inhibited the LF-induced upregulation of MMP2 and MMP9 expression. The findings also demonstrated that PSP could markedly reduce circulating Col IV levels, suggesting its potential to repair the vascular endothelial basement membrane and alleviate LF-induced damage.

LF development is a complex process involving interactions between HSCs, KCs, hepatocytes and hepatic sinusoidal endothelial cells (50). KCs have a notable role as inflammatory cells. In experimental LF models, KC infiltration typically precedes the activation of HSCs, with conditioned cultures of KCs from both normal and LF rats promoting HSC activation (51,52). The interaction between HSCs and KCs is mediated by various humoral transmitters, including chemokines, cytokines and intercellular adhesion molecules (53). This is consistent with the findings of the present study. The present study observed significant increases in the levels of proinflammatory factors and peroxidases, as well as reductions in the levels of anti-inflammatory factors and antioxidant enzymes, in the serum of LF rats. These changes were reversed by PSP. These results suggested that PSP may help protect KCs from LF-induced damage, reducing both inflammation and oxidative stress.

Sustained activation of HSCs is a key step in LF progression. After liver injury, the combined effects of paracrine cytokines and autocrine signaling from HSCs lead to HSC proliferation, cytosolic enlargement, disappearance of vitamin A droplets and increased ECM accumulation, and induce the expression of α-SMA, a marker of activated HSCs with contractile function (54-56). The findings of the present study revealed that PSP significantly reduced α-SMA levels in LF, suggesting that PSP may inhibit HSC activation. Furthermore, the TGF-β/Smad signaling pathway was investigated. TGF-β is secreted not only by HSCs but also by KCs, hepatic sinusoidal endothelial cells and inflammatory cells surrounding the LF (57,58). HSCs are not only sources but also primary targets of TGF-β. Secreted TGF-β promotes a positive feedback loop, enhancing the synthesis and secretion of more TGF-β by surrounding HSCs, thereby increasing HSC activation. TGF-β also promotes the synthesis of α-SMA and the ECM by HSCs (59). Among the three isoforms of TGF-β, TGF-β1, TGF-β2 and TGF-β3, TGF-β1 is most closely associated with LF. Its downstream Smad proteins regulate LF through TGF-β1 binding, phosphorylation and nuclear translocation (60). The results of the present study indicated that PSP can significantly modulate the TGF-β/Smad signaling pathway, suggesting that PSP may regulate this pathway by inhibiting HSC activation, reducing ECM deposition and exerting anti-LF effects.

However, the present study has several limitations. In the present study, PSP treatment significantly attenuated α-SMA expression and inflammatory responses, possibly through modulating HSC activation and KC function; however, the exact mechanisms require elucidation. Further research should focus on HSCs and KCs to improve understanding of the mechanisms underlying the anti-LF effects of PSP. After fully elucidating the mechanism of PSP in combating LF, whether combining natural anti-fibrotic drugs (such as PSP) with interventions targeting complementary pathways can provide additional benefits for LF and glucose homeostasis will be explored (61).

In conclusion, in the current study PSP significantly improved liver function, reduced collagen fiber deposition while repairing the hepatic vascular basement membrane, and alleviated the inflammatory and oxidative responses induced by LF. These effects may be associated with the regulation of the TGF-β/Smad signaling pathway.

Acknowledgements

Not applicable.

Funding

The present study was supported by the Yunnan Fundamental Research Projects (grant no. 202401AU070034); *Populus euphratica* Talents-Introduction of Talents Research Launch Project (grant no. TDZKSS202553) and the Yunnan Fundamental Research Projects (grant no. 202201AT070284).

Availability of data and materials

The data generated in the present study may be requested from the corresponding author.

Authors' contributions

XL, TZ and YL performed experiments. YY and MG wrote the manuscript. XL, TZ, YY and MG contributed to analysis and interpretation of data. YL provided critical comments on the revision of the manuscript. MG, YL and ZZ contributed to the conception, design and supervision of the study. MG, YY and YL provided funding. MG and YY confirm the authenticity of all the raw data. All authors read and approved the final version of the manuscript.

Ethics approval and consent to participate

All animal procedures were approved by the Animal Ethics Committee of Heilongjiang University of Chinese Medicine (approval no. 2021101101; Harbin, China).

Patient consent for publication

Not applicable.

Competing interests

The authors declare that they have no competing interests.

References

1. Pei Q, Yi Q and Tang L: liver fibrosis resolution: From molecular mechanisms to therapeutic opportunities. Int J Mol Sci 24: 9671, 2023.
2. Kaps L and Schuppan D: Targeting cancer associated fibroblasts in liver fibrosis and liver cancer using nanocarriers. Cells 9: 2027, 2020.
3. Yuan S, Wei C, Liu G, Zhang L, Li J, Li L, Cai S and Fang L: Sorafenib attenuates liver fibrosis by triggering hepatic stellate cell ferroptosis via HIF-1α/SLC7A11 pathway. Cell Prolif 55: e13158, 2022.
4. Hammerich L and Tacke F: Hepatic inflammatory responses in liver fibrosis. Nat Rev Gastroenterol Hepatol 20: 633-646, 2023.
5. Fu Y, Zhou X, Wang L, Fan W, Gao S, Zhang D, Ling Z, Zhang Y, Ma L, Bai F, *et al*: Salvianolic acid B attenuates liver fibrosis by targeting Ecm1 and inhibiting hepatocyte ferroptosis. Redox Biol 69: 103029, 2024.
6. Crouchet E, Dachraoui M, Juhling F, Roehlen N, Oudot MA, Durand SC, Ponsolles C, Gadenne C, Meiss-Heydmann L, Moehlin J, *et al*: Targeting the liver clock improves fibrosis by restoring TGF-β signaling. J Hepatol 82: 120-133, 2025.
7. Song Y, Wei J, Li R, Fu R, Han P, Wang H, Zhang G, Li S, Chen S, Liu Z, *et al*: Tyrosine kinase receptor B attenuates liver fibrosis by inhibiting TGF-β/SMAD signaling. Hepatology 78: 1433-1447, 2023.
8. Yang Y, Sun M, Li W, Liu C, Jiang Z, Gu P, Li J, Wang W, You R, Ba Q, *et al*: Rebalancing TGF-β/Smad7 signaling via Compound kushen injection in hepatic stellate cells protects against liver fibrosis and hepatocarcinogenesis. Clin Transl Med 11: e410, 2021.
9. Zhang L, Liu C, Yin L, Huang C and Fan S: Mangiferin relieves CCl4-induced liver fibrosis in mice. Sci Rep 13: 4172, 2023.
10. Cheng Q, Li C, Yang CF, Zhong YJ, Wu D, Shi L, Chen L, Li YW and Li L: Methyl ferulic acid attenuates liver fibrosis and hepatic stellate cell activation through the TGF-β1/Smad and NOX4/ROS pathways. Chem Biol Interact 299: 131-139, 2019.
11. Liao YJ, Lee CY, Twu YC, Suk FM, Lai TC, Chang YC, Lai YC, Yuan JW, Jhuang HM, Jian HR, *et al*: Isolation and biological evaluation of Alfa-mangostin as potential therapeutic agents against liver fibrosis. Bioengineering (Basel) 10: 1075, 2023.
12. Hernandez-Aquino E, Zarco N, Casas-Grajales S, Ramos-Tovar E, Flores-Beltran RE, Arauz J, Shibayama M, Favari L, Tsutsumi V, Segovia J and Muriel P: Naringenin prevents experimental liver fibrosis by blocking TGFβ-Smad3 and JNK-Smad3 pathways. World J Gastroenterol 23: 4354-4368, 2017.
13. Liu H, Yue L, Li Y, Zheng T, Zhang W, Li C, Zhuang W and Fan L: Combination of Polygonatum Rhizoma and Scutellaria baicalensis triggers apoptosis through downregulation of PON(3)-induced mitochondrial damage and endoplasmic reticulum stress in A549 cells. Environ Toxicol 39: 3172-3187, 2024.
14. Chen X, Tong YL, Ren ZM, Chen SS, Mei XY, Zhou QY and Dai GH: Hypoglycemic mechanisms of *Polygonatum sibiricum* polysaccharide in db/db mice via regulation of glycolysis/gluconeogenesis pathway and alteration of gut microbiota. Heliyon 9: e15484, 2023.
15. Chen W, Shen Z, Dong W, Huang G, Yu D, Chen W, Yan X and Yu Z: *Polygonatum sibiricum* polysaccharide ameliorates skeletal muscle aging via mitochondria-associated membrane-mediated calcium homeostasis regulation. Phytomedicine 129: 155567, 2024.
16. Wang T, Li YQ, Yu LP, Zi L, Yang YQ, Zhang M, Hao JJ, Gu W, Zhang F, Yu J and Yang XX: Compatibility of Polygonati Rhizoma and Angelicae Sinensis Radix enhance the alleviation of metabolic dysfunction-associated fatty liver disease by promoting fatty acid beta-oxidation. Biomed Pharmacother 162: 114584, 2023.
17. Mu JK, Zi L, Li YQ, Yu LP, Cui ZG, Shi TT, Zhang F, Gu W, Hao JJ, Yu J and Yang XX: Jiuzhuan Huangjing Pills relieve mitochondrial dysfunction and attenuate high-fat diet-induced metabolic dysfunction-associated fatty liver disease. Biomed Pharmacother 142: 112092, 2021.
18. Liu J, Zhang H, Ji B, Cai S, Wang R, Zhou F, Yang J and Liu H: A diet formula of Puerariae radix, Lycium barbarum, Crataegus pinnatifida, and Polygonati rhizoma alleviates insulin resistance and hepatic steatosis in CD-1 mice and HepG2 cells. Food Funct 5: 1038-1049, 2014.
19. Gong H, Gan X, Qin B, Chen J, Zhao Y, Qiu B, Chen W, Yu Y, Shi S, Li T, *et al*: Structural characteristics of steamed Polygonatum cyrtonema polysaccharide and its bioactivity on colitis via improving the intestinal barrier and modifying the gut microbiota. Carbohydr Polym 327: 121669, 2024.
20. Zhong R, Shen L, Fan Y, Luo Q, Hong R, Sun X, Zhou X and Wan J: Anti-aging mechanism and effect of treatment with raw and wine-steamed *Polygonatum sibiricum* on D-galactose-induced aging in mice by inhibiting oxidative stress and modulating gut microbiota. Front Pharmacol 15: 1335786, 2024.
21. Li H: Advances in anti hepatic fibrotic therapy with Traditional Chinese Medicine herbal formula. J Ethnopharmacol 251: 112442, 2020.
22. Ji D, Chen Y, Bi J, Shang Q, Liu H, Wang JB, Tan L, Wang J, Chen Y, Li Q, *et al*: Entecavir plus Biejia-Ruangan compound reduces the risk of hepatocellular carcinoma in Chinese patients with chronic hepatitis B. J Hepatol 77: 1515-1524, 2022.
23. Shen B, Deng L, Liu Y, Li R, Shen C, Liu X, Li Y and Yuan H: Effects of novel Fufang Biejia Ruangan Tablets with sheep placenta as substitute for *Hominis Placenta* on CCl_4-induced liver fibrosis. Chin Herb Med 14: 104-110, 2022.
24. Chinese Pharmacopoeia Commission: Pharmacopoeia of the People's Republic of China (2015 Edition). Beijing China Medical Science Press 1: 306-307, 2015.
25. Staub F, Tournoux-Facon C, Roumy J, Chaigneau C, Morichaut-Beauchant M, Levillain P, Prevost C, Aube C, Lebigot J, Oberti F, *et al*: Liver fibrosis staging with contrast-enhanced ultrasonography: Prospective multicenter study compared with METAVIR scoring. Eur Radiol 19: 1991-1997, 2009.

26. Livak KJ and Schmittgen TD: Analysis of relative gene expression data using real-time quantitative PCR and the 2(-Delta Delta C(T)) method. Methods 25: 402-408, 2001.
27. Guan Y, Enejder A, Wang M, Fang Z, Cui L, Chen SY, Wang J, Tan Y, Wu M, Chen X, *et al*: A human multi-lineage hepatic organoid model for liver fibrosis. Nat Commun 12: 6138, 2021.
28. Xia Y, Yu B, Ma C, Tu Y, Zhai L, Yang Y, Liu D, Liu Y, Wu H, Dan H and You P: Yu Gan Long reduces rat liver fibrosis by blocking TGF-β1/Smad pathway and modulating the immunity. Biomed Pharmacother 106: 1332-1338, 2018.
29. Mak KM and Mei R: Basement membrane type IV collagen and laminin: An overview of their biology and value as fibrosis biomarkers of liver disease. Anat Rec (Hoboken) 300: 1371-1390, 2017.
30. Meng X, Kuang H, Wang Q, Zhang H, Wang D and Kang T: A polysaccharide from Codonopsis pilosula roots attenuates carbon tetrachloride-induced liver fibrosis via modulation of TLR4/NF-κB and TGF-β1/Smad3 signaling pathway. Int Immunopharmacol 119: 110180, 2023.
31. Tong G, Chen X, Lee J, Fan J, Li S, Zhu K, Hu Z, Mei L, Sui Y, Dong Y, *et al*: Fibroblast growth factor 18 attenuates liver fibrosis and HSCs activation via the SMO-LATS1-YAP pathway. Pharmacol Res 178: 106139, 2022.
32. Chen C, Chen J, Wang Y, Fang L, Guo C, Sang T, Peng H, Zhao Q, Chen S, Lin X and Wang X: Ganoderma lucidum polysaccharide inhibits HSC activation and liver fibrosis via targeting inflammation, apoptosis, cell cycle, and ECM-receptor interaction mediated by TGF-β/Smad signaling. Phytomedicine 110: 154626, 2023.
33. Bai J, Qian B, Cai T, Chen Y, Li T, Cheng Y, Wu Z, Liu C, Ye M, Du Y and Fu W: Aloin attenuates oxidative stress, inflammation, and CCl_4-induced liver fibrosis in mice: Possible role of TGF-β/Smad signaling. J Agric Food Chem 71: 19475-19487, 2023.
34. Jiang Y, Zeng X, Dai H, Luo S and Zhang X: *Polygonatum sibiricum* polysaccharide regulation of gut microbiota: A viable approach to alleviate cognitive impairment. Int J Biol Macromol 277: 134494, 2024.
35. Jiang Q, Lv Y, Dai W, Miao X and Zhong D: Extraction and bioactivity of polygonatum polysaccharides. Int J Biol Macromol 54: 131-135, 2013.
36. Bi J, Zhao C, Jin W, Chen Q, Fan B and Qian C: Study on pharmacokinetics and tissue distribution of *Polygonatum sibiricum* polysaccharide in rats by fluorescence labeling. Int J Biol Macromol 215: 541-549, 2022.
37. Liu R, Zhang X, Cai Y, Xu S, Xu Q, Ling C, Li X, Li W, Liu P and Liu W: Research progress on medicinal components and pharmacological activities of *Polygonatum sibiricum*. J Ethnopharmacol 328: 118024, 2024.
38. Xue X, Li Y, Zhang S, Yao Y, Peng C and Li Y: Hydroxysafflor yellow A exerts anti-fibrotic and anti-angiogenic effects through miR-29a-3p/PDGFRB axis in liver fibrosis. Phytomedicine 132: 155830, 2024.
39. Zhang Q, Shang MM, Ling QF, Wu XP and Liu CY: Hepatoprotective effects of loach (Misgurnus anguillicaudatus) lyophilized powder on dimethylnitrosamine-induced liver fibrosis in rats. Arch Pharm Res 44: 1-12, 2021.
40. Leroy V, Monier F, Bottari S, Trocme C, Sturm N, Hilleret MN, Morel F and Zarski JP: Circulating matrix metalloproteinases 1, 2, 9 and their inhibitors TIMP-1 and TIMP-2 as serum markers of liver fibrosis in patients with chronic hepatitis C: Comparison with PIIINP and hyaluronic acid. Am J Gastroenterol 99: 271-279, 2004.
41. Li G, Lin J, Peng Y, Qin K, Wen L, Zhao T and Feng Q: Curcumol may reverse early and advanced liver fibrogenesis through downregulating the uPA/uPAR pathway. Phytother Res 34: 1421-1435, 2020.
42. Wang Y, Liu Y, Liu Y, Zhong J, Wang J, Sun L, Yu L, Wang Y, Li Q, Jin W and Yan Z: Remodeling liver microenvironment by L-arginine loaded hollow polydopamine nanoparticles for liver cirrhosis treatment. Biomaterials 295: 122028, 2023.
43. Li H: Intercellular crosstalk of liver sinusoidal endothelial cells in liver fibrosis, cirrhosis and hepatocellular carcinoma. Dig Liver Dis 54: 598-613, 2022.
44. Parola M and Pinzani M: Liver fibrosis: Pathophysiology, pathogenetic targets and clinical issues. Mol Aspects Med 65: 37-55, 2019.
45. Parola M and Pinzani M: Liver fibrosis in NAFLD/NASH: From pathophysiology towards diagnostic and therapeutic strategies. Mol Aspects Med 95: 101231, 2024.
46. Bataller R and Brenner DA: Liver fibrosis. J Clin Invest 115: 209-218, 2005.
47. Kamm DR and McCommis KS: Hepatic stellate cells in physiology and pathology. J Physiol 600: 1825-1837, 2022.
48. Zhang L, Shi J, Shen Q, Fu Y, Qi S, Wu J, Chen J, Zhang H, Mu Y, Chen G, *et al*: Astragalus saponins protect against extrahepatic and intrahepatic cholestatic liver fibrosis models by activation of farnesoid X receptor. J Ethnopharmacol 318: 116833, 2024.
49. Naim A, Pan Q and Baig MS: Matrix Metalloproteinases (MMPs) in liver diseases. J Clin Exp Hepatol 7: 367-372, 2017.
50. Pastore M, Caligiuri A, Raggi C, Navari N, Piombanti B, Di Maira G, Rovida E, Piccinni MP, Lombardelli L, Logiodice F, *et al*: Macrophage MerTK promotes profibrogenic cross-talk with hepatic stellate cells via soluble mediators. JHEP Rep 4: 100444, 2022.
51. Wu P, Luo X, Sun M, Sun B and Sun M: Synergetic regulation of kupffer cells, extracellular matrix and hepatic stellate cells with versatile CXCR4-inhibiting nanocomplex for magnified therapy in liver fibrosis. Biomaterials 284: 121492, 2022.
52. Takemura S, Azuma H, Osada-Oka M, Kubo S, Shibata T and Minamiyama Y: S-allyl-glutathione improves experimental liver fibrosis by regulating Kupffer cell activation in rats. Am J Physiol Gastrointest Liver Physiol 314: G150-G163, 2018.
53. Zhang Z, Yuan Y, Hu L, Tang J, Meng Z, Dai L, Gao Y, Ma S, Wang X, Yuan Y, *et al*: ANGPTL8 accelerates liver fibrosis mediated by HFD-induced inflammatory activity via LILRB2/ERK signaling pathways. J Adv Res 47: 41-56, 2023.
54. Cogliati B, Yashaswini CN, Wang S, Sia D and Friedman SL: Friend or foe? The elusive role of hepatic stellate cells in liver cancer. Nat Rev Gastroenterol Hepatol 20: 647-661, 2023.
55. Zhu Y, Kang A, Kuai Y, Guo Y, Miao X, Zhu L, Kong M and Li N: The chromatin remodeling protein BRG1 regulates HSC-myofibroblast differentiation and liver fibrosis. Cell Death Dis 14: 826, 2023.
56. Pydyn N, Ferenc A, Trzos K, Pospiech E, Wilamowski M, Mucha O, Major P, Kadluczka J, Rodrigues PM, Banales JM, *et al*: MCPIP1 inhibits hepatic stellate cell activation in autocrine and paracrine manners, preventing liver fibrosis. Cell Mol Gastroenterol Hepatol 17: 887-906, 2024.
57. Dewidar B, Meyer C, Dooley S and Meindl-Beinker AN: TGF-β in hepatic stellate cell activation and liver fibrogenesis-updated 2019. Cells 8: 1419, 2019.
58. Sun L, Wang Y, Wang X, Navarro-Corcuera A, Ilyas S, Jalan-Sakrikar N, Gan C, Tu X, Shi Y, Tu K, *et al*: PD-L1 promotes myofibroblastic activation of hepatic stellate cells by distinct mechanisms selective for TGF-β receptor I versus II. Cell Rep 38: 110349, 2022.
59. Pan Q, Gao M, Kim D, Ai W, Yang W, Jiang W, Brashear W, Dai Y, Li S, Sun Y, *et al*: Hepatocyte FoxO1 deficiency protects from liver fibrosis via reducing inflammation and TGF-β1-mediated HSC activation. Cell Mol Gastroenterol Hepatol 17: 41-58, 2024.
60. Shu G, Yusuf A, Dai C, Sun H and Deng X: Piperine inhibits AML-12 hepatocyte EMT and LX-2 HSC activation and alleviates mouse liver fibrosis provoked by CCl_4: Roles in the activation of the Nrf2 cascade and subsequent suppression of the TGF-β1/Smad axis. Food Funct 12: 11686-11703, 2021.
61. Song K, Kong X, Xian Y, Yu Z, He M, Xiao D, Liang D, Zhang Z, Liu T, Huang Z, *et al*: Roux-en-Y gastric bypass improves liver and glucose homeostasis in Zucker diabetic fatty rats by upregulating hepatic trefoil factor family 3 and activating the phosphatidylinositol 3-kinase/protein kinase B pathway. Surg Obes Relat Dis: Jan 10, 2025 doi: 10.1016/j.soard.2024.12.024 (Epub ahead of print).